Supplementary Material

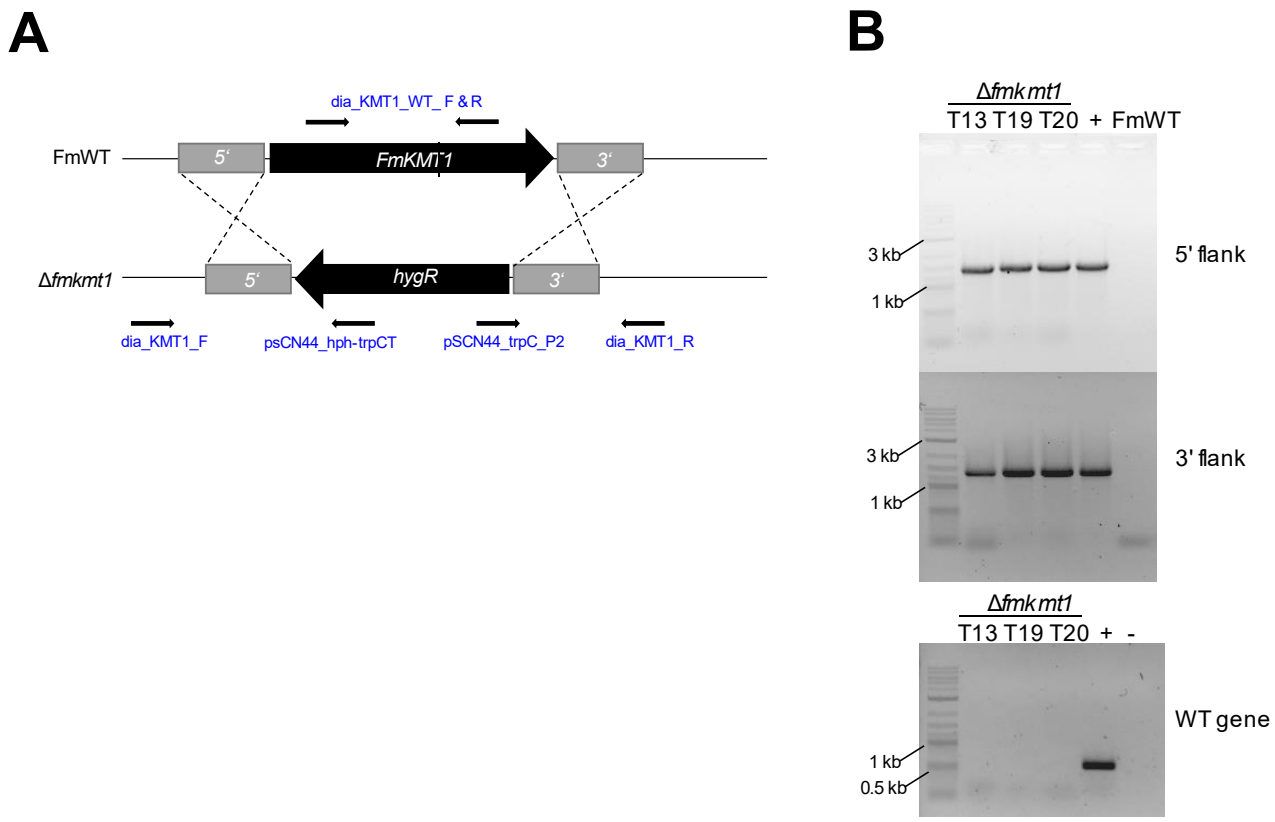

Figure S1: Strategy and verification of Δ*fmkmt1* deletion mutants by diagnostic PCR. (A) Deletion and verification strategy of Δ*fmkmt1* mutants. Primer pairs for diagnostic PCRs are depicted in blue. **(B)** Verification of deletion *via* homologous recombination with the hygR cassette. Homologous integration was verified by the presence of the upstream region (5' flank) with the primers Dia_FmKMT1_F//pCSN44_hph-trpC-T and the downstream region (3' flank) by Dia_FmKMT1_R//pCSN44_trpC_P2. Absence of wild-type gene was checked with Dia_WTKMT1_F//R for three independent transformants Δ*fmkmt1* T13, T19 and T20. For 5' and 3' Δ*fmkmt1* gDNA prior single spore isolation was used as positive control (+), while FmWT gDNA served as + control for wild-type (WT) gene diagnostic PCR. As size marker 1 kb Plus DNA ladder (NEB) was used.

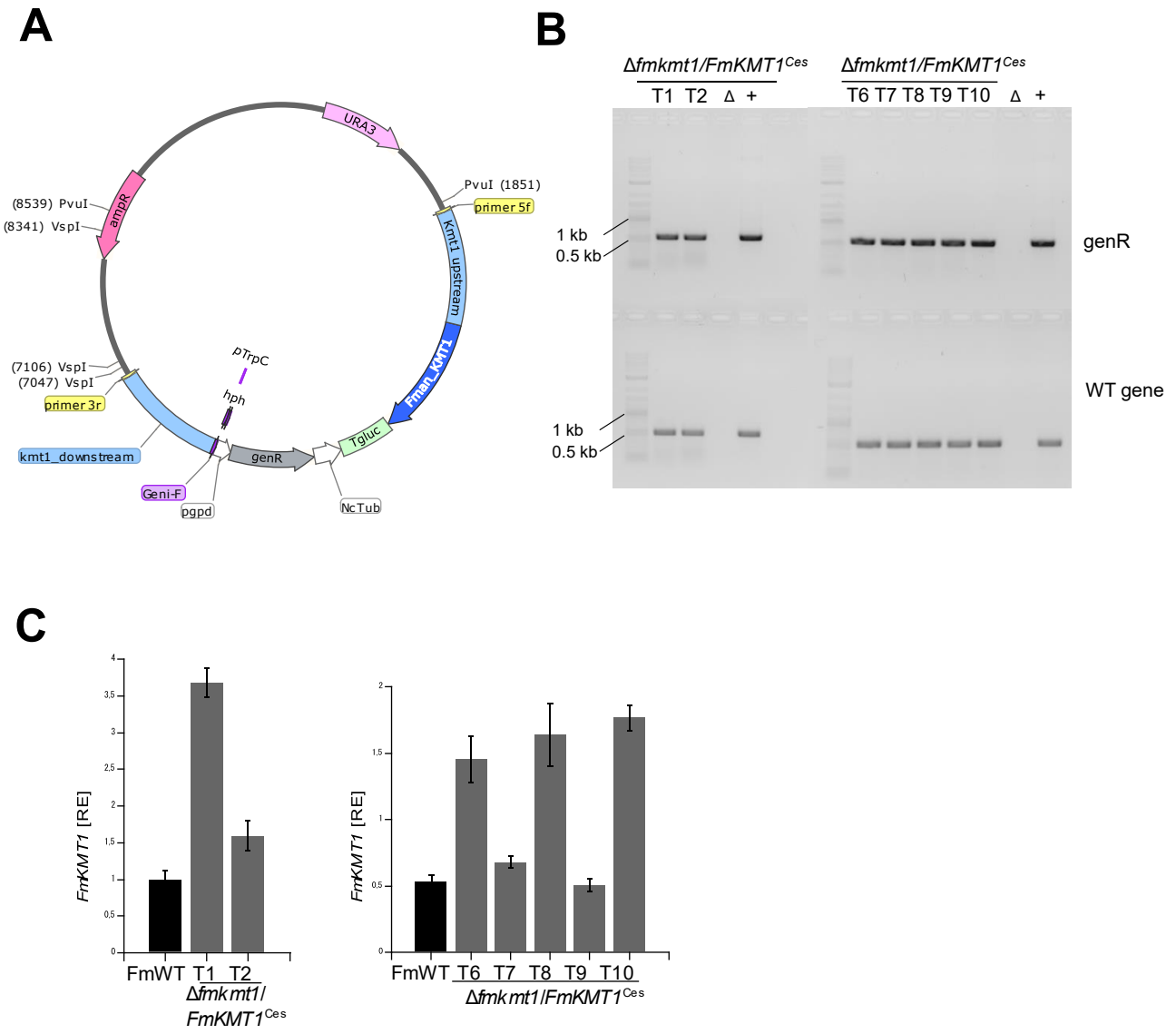

Figure S2: Complementation strategy and verification of Δ*fmkmt1*/*FmKMT1*^{Ces} by diagnostic PCR. (A) Strategy for complementation of Δ*fmkmt1*_T19. Enzymes used for restriction are shown. **(B)** Verification of gained transformants. Complementation was achieved by *ex-situ* integration of the native *FmKMT1* wild-type gene of *F. mangiferae* MRC7560 (FmWT) into Δ*fmkmt1* T19. Genomic DNA was isolated from overall seven geneticin-resistant transformants and correct re-integration of the native *FmKMT1* was verified by diagnostic PCR. For this, the amplification of the genR cassette (GeniTglucR/GeniF) together with the wild-type *FmKMT1* gene was performed using the primer pair Dia_WTKMT1F//R. As negative control gDNA of the recipient Δ*fmkmt1* T19 strain was used, while as positive control (+) for geneticin resistance the pΔ*fmkmt1*/*FmKMT1*^{Ces} was used. For wild-type gene amplification FmWT gDNA served as + control. As size marker 1 kb Plus DNA ladder (NEB) was used. **(C)** *FmKMT1* transcript levels in complemented strains. To evaluate suitability of the gained complementation strains, *FmKMT1* transcript levels were assessed by RT-qPCR after 3 days of growth on solid CM. Data represent mean values (n = x).

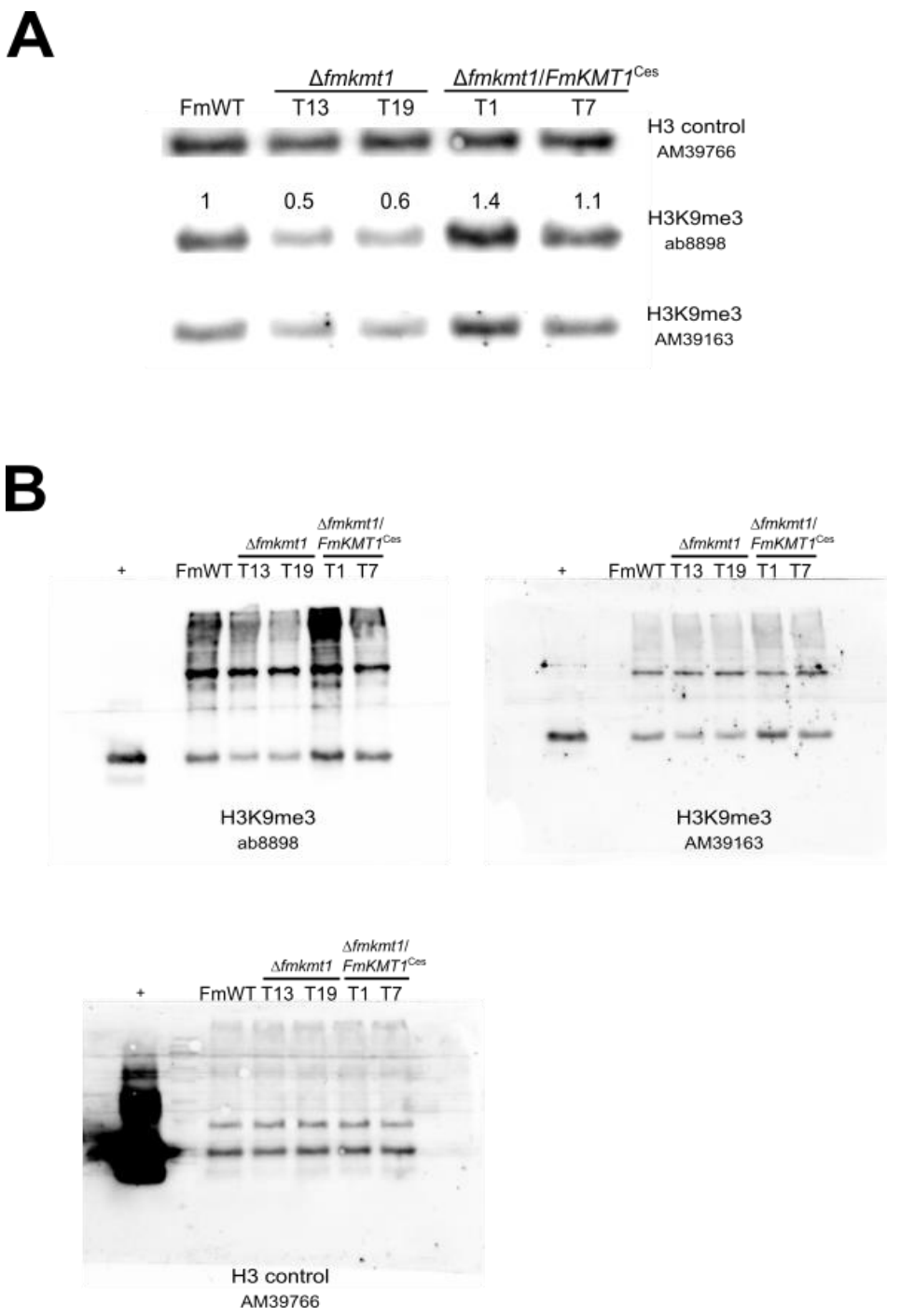

Figure S3: Lack of *FmKMT1* results in reduced overall H3K9me3 in *Fusarium mangiferae*. (A) Cropped images of the relevant H3 histone signals as determined by western blotting. For analysis, the *F. mangiferae* wild-type strain (FmWT), the Δ*fmkmt1* and complemented Δ*fmkmt1*/*FmKMT1*^{Ces} strains were grown in liquid ICI medium supplemented with 120 mM $NaNO_3$ for 4 days. Whole proteins were extracted, and 30 µg were separated on a SDS acrylamide gel. Overall H3K9me3 levels were determined using two different anti-H3K9me3 (AB, Abcam; AM, Active Motif), and an anti-H3 C-term-specific antibody was used for referencing. As positive (+) control histones from calf thymus were used. **(B)** Uncropped western blot membranes.

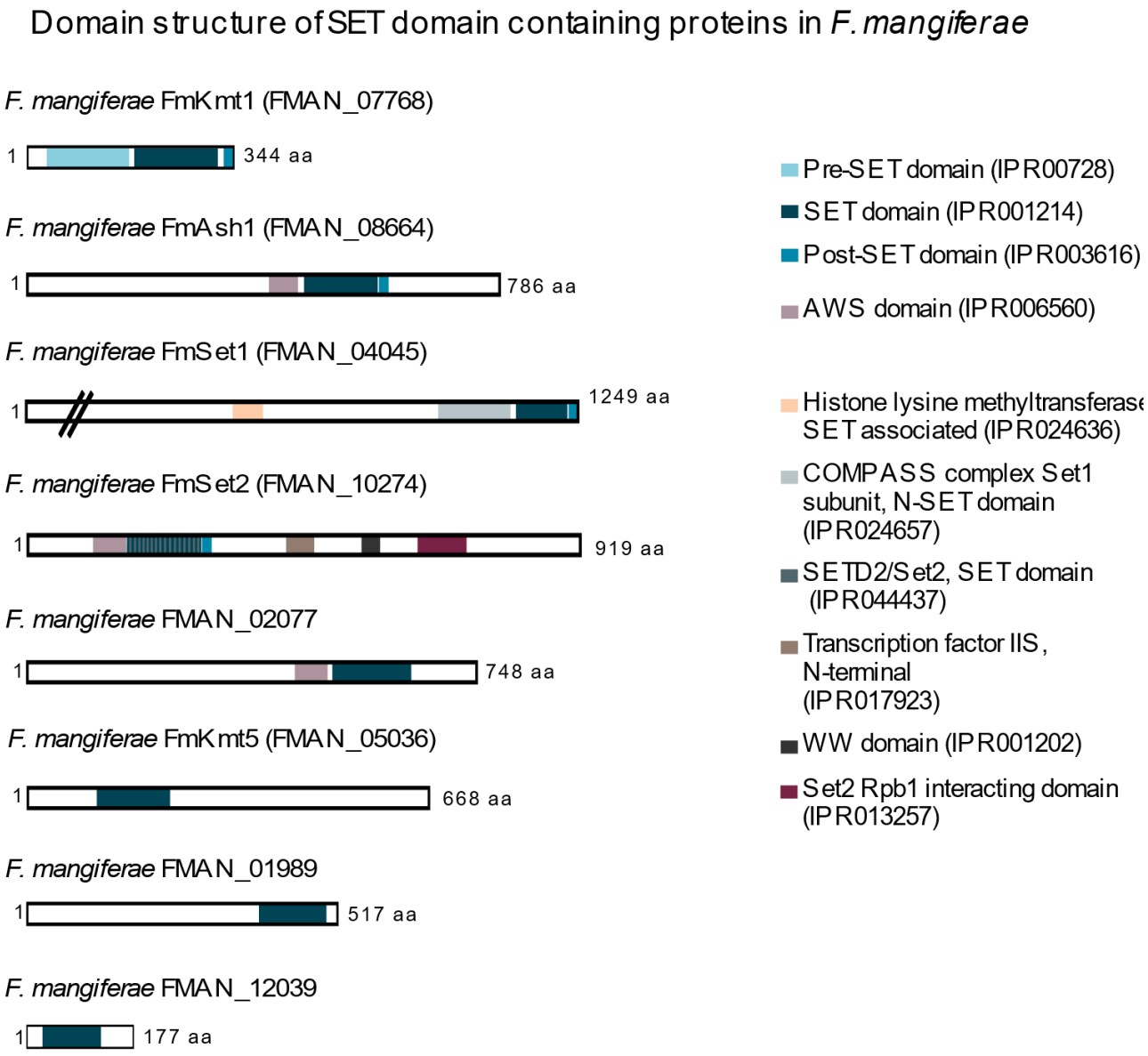

Figure S4: Domain structures of SET domain containing proteins in *F. mangiferae* (FmWT). pBLAST search of FmKmt1 SET-domain against FmWT genome. The pBLAST search revealed seven additional SET-domain containing proteins with similarity to FmKmt1 SET-domain. Protein sequences were retrieved from NCBI and subsequently the domain organization was analyzed using InterPro (Blum et al., 2021)**.** The InterPro accsession numbers are shown in the figure legend**.**

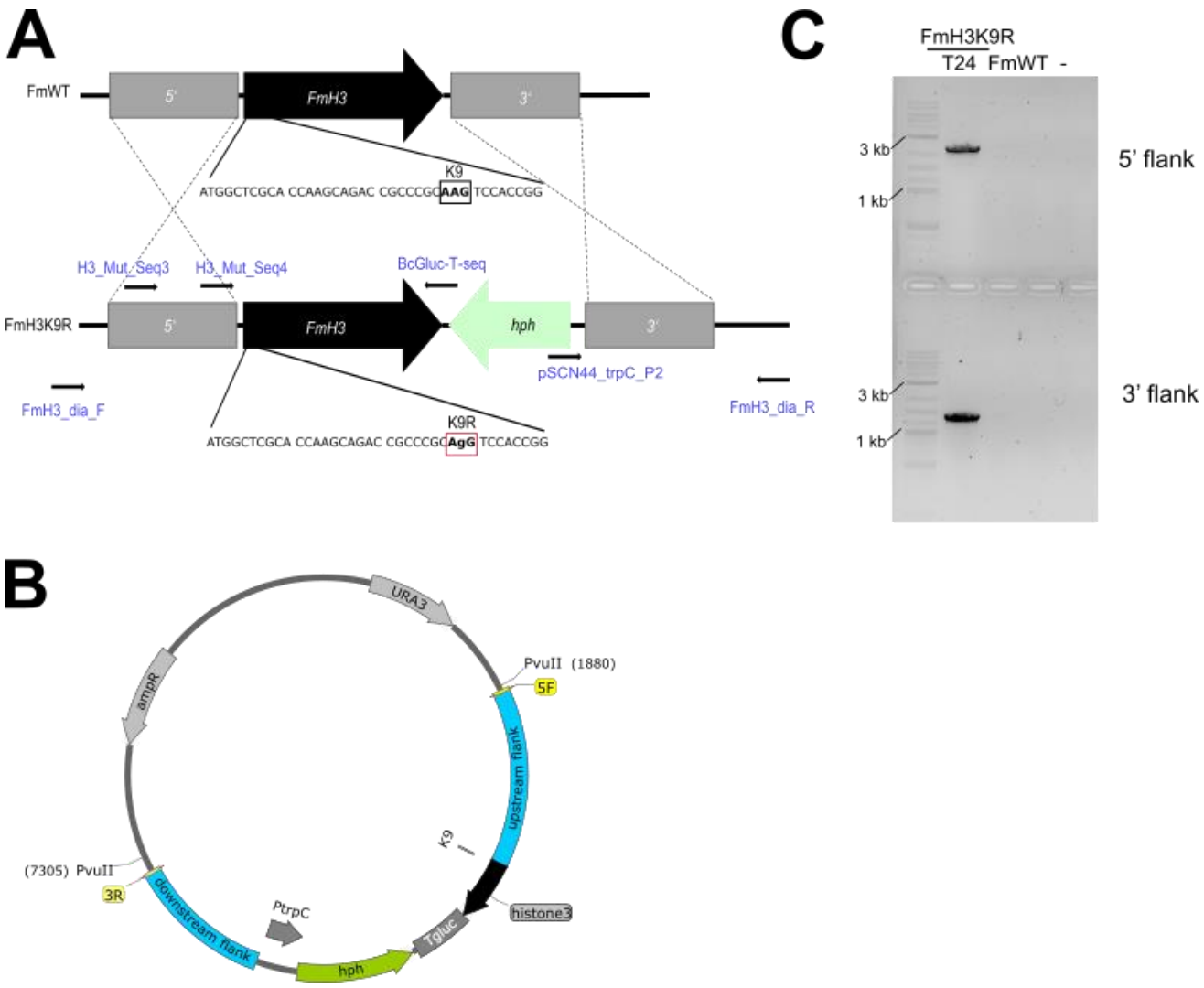

Figure S5: Strategy, plasmid map and verification of H3K9R mutants by diagnostic PCR and sequencing. (A) Verification strategy of lysine 9 (K9) to arginine 9 (R9) point mutation. Primer pairs for diagnostic PCRs as well as sequencing are designated in blue. **(B)** FmH3K9R plasmid map. Enzyme used for restriction prior to transformation are shown. **(C)**Verification of successful integration *via* homologous recombination. Homologous integration was verified by the presence of the upstream region (5' flank) with the primer pair FmH3_dia_F//BcGluc-T-seq and the downstream region (3' flank) with FmH3_dia_R//pCSN44_trpC_P2. Successful amino acid exchange was verified by sequencing with the primer pair H3_Mut_Seq3//BcGluc-T-seq for template generation and H3_Mut_Seq4 for sequencing analysis. As size marker 1 kb Plus DNA ladder (NEB) was used. As negative (–) control sterile water was used.

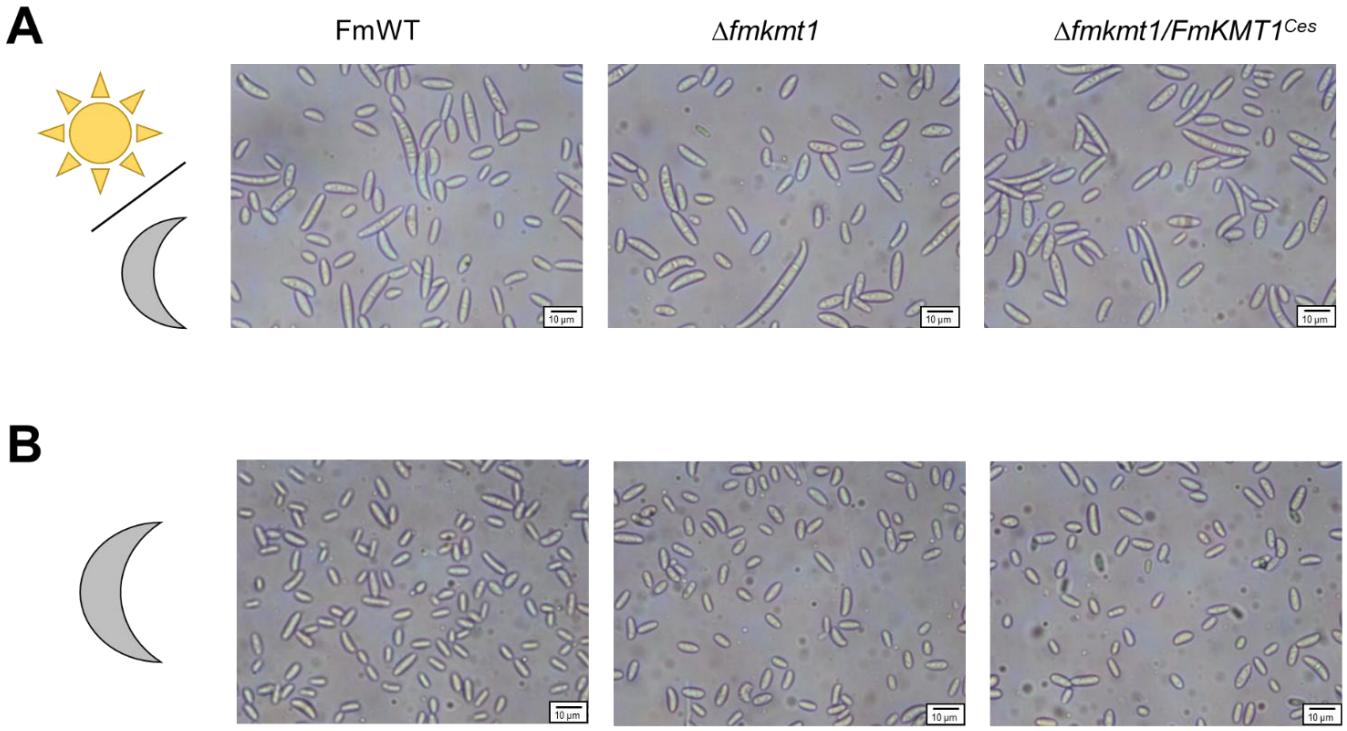

Figure S6: Conidia production of *F. mangiferae* (FmWT), Δ*fmkmt1* and Δ*fmkmt1*/*FmKMT1*^{Ces} associated mutant strains under light and dark (L/D) and dark (D) conditions. FmWT, Δ*fmkmt1* and Δ*fmkmt1*/*FmKMT1*^{Ces} were incubated for 7 days on V8 vegetable juice media with **(A)** 16 h light and 8 h dark cycle (L/D), or **(B)** in complete darkness (D). Conidia were observed under light microscope with 40x magnitude. Black bars indicate 10 µm.

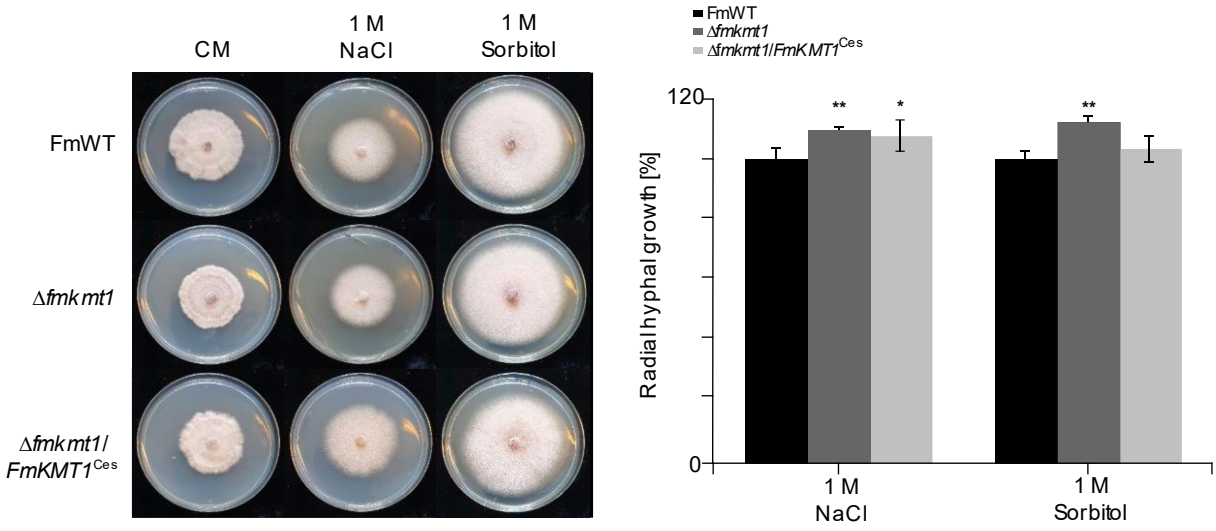

Figure S7: Involvement of FmKmt1 in osmotic stress response. Radial hyphal growth of *F. mangiferae* wild-type strain (FmWT), Δ*fmkmt1* and Δ*fmkmt1*/*FmKMT1*^{Ces} on complete medium supplemented with either 1 M NaCl or 1 M sorbitol as compared to unsupplemented CM. Strains were grown for 7 days at 30 °C in the dark. The experiments were performed in technical triplicates and biological duplicates. Hyphal growth of FmWT on the respective media was arbitrarily set to 100%. Growth on media supplemented with stressors was adjusted to normal growth on CM plates of the respective strain. Mean values and standard deviations are given in the diagram. For statistical analysis a student's *t* test was performed. Asterisks above the bars denote significant differences in the radial hyphal growth production of the indicated strains compared to the respective wild-type, * $p<0.05$; ** $p<0.001$.

	60 mM gln	6 mM gln	6 mM $NaNO_3$
Fusaric acid	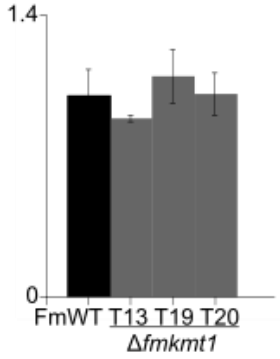	n.d.	n.d.
Bikaverin	n.d.	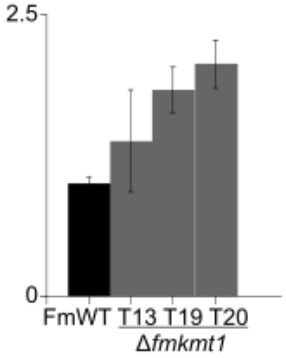	n.d.
Beauvericin	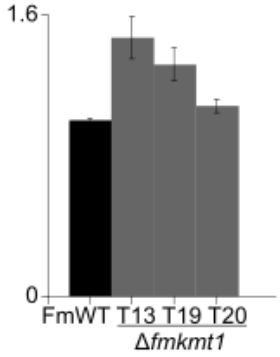	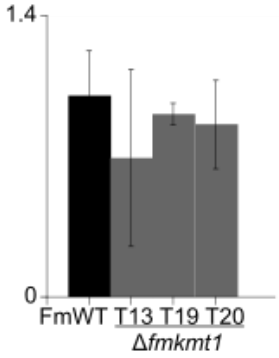	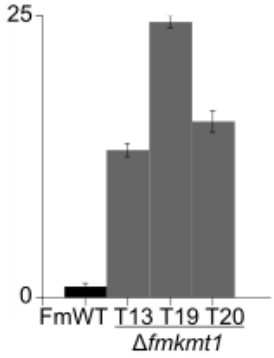
Fusarubins	n.d.	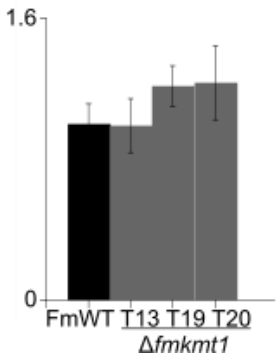	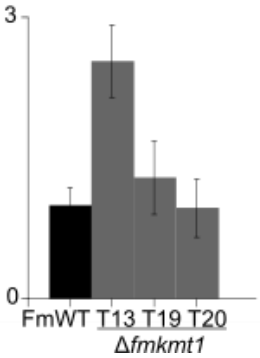

Figure S8: Quantification of known SMs produced by *F. mangiferae* under standard laboratory conditions. SM production of the *F. mangiferae* wild-type strain (FmWT) and three independent Δ*fmkmt1* mutant strains was quantified using HPLC-HRMS. For this, FmWT and *fmkmt1* deletion strains were cultivated in liquid ICI supplemented with either 60 mM or 6 mM glutamine (gln) and 6 mM $NaNO_3$ for 7 days at 30 °C in constant darkness. Experiments were performed in biological and technical triplicates. Mean values and standard deviations are shown in the diagram. For comparison reasons the wild type was set to 1. n.d., not detected in the supernatant.

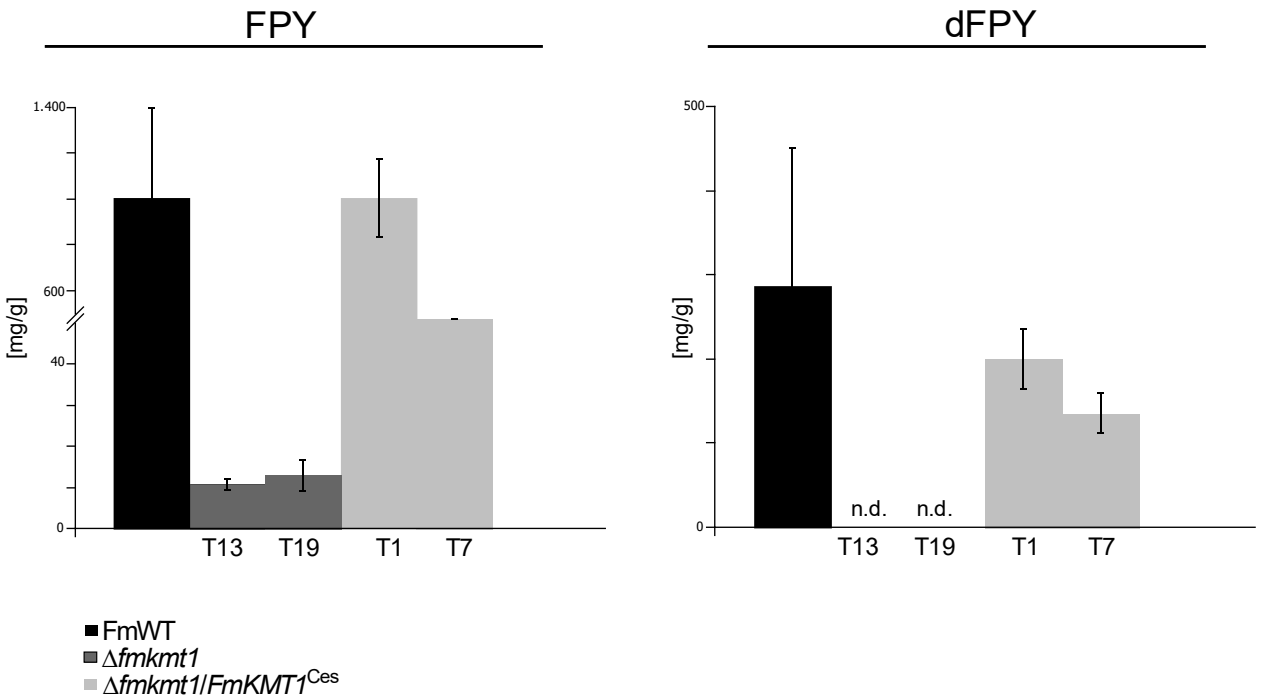

Figure S9: Quantification of fusapyrone (FPY) and deoxyfusapyrone (dFPY) in *F. mangiferae*. FPY and dFPY production of the *F. mangiferae* wild-type strain (FmWT), the Δ*fmkmt1* and the Δ*fmkmt1*/*FmKMT1*^{Ces} strains quantified with HPLC-HRMS. For this, indicated fungal strains were grown in liquid ICI supplemented 6 mM $NaNO_3$ for 7 days at 30 °C in constant darkness. The supernatant was directly applied for quantitative analysis. Experiments were performed in in technical triplicates and biological duplicates. Mean values and standard deviations are shown in diagram. n.d., not detected in the supernatant.

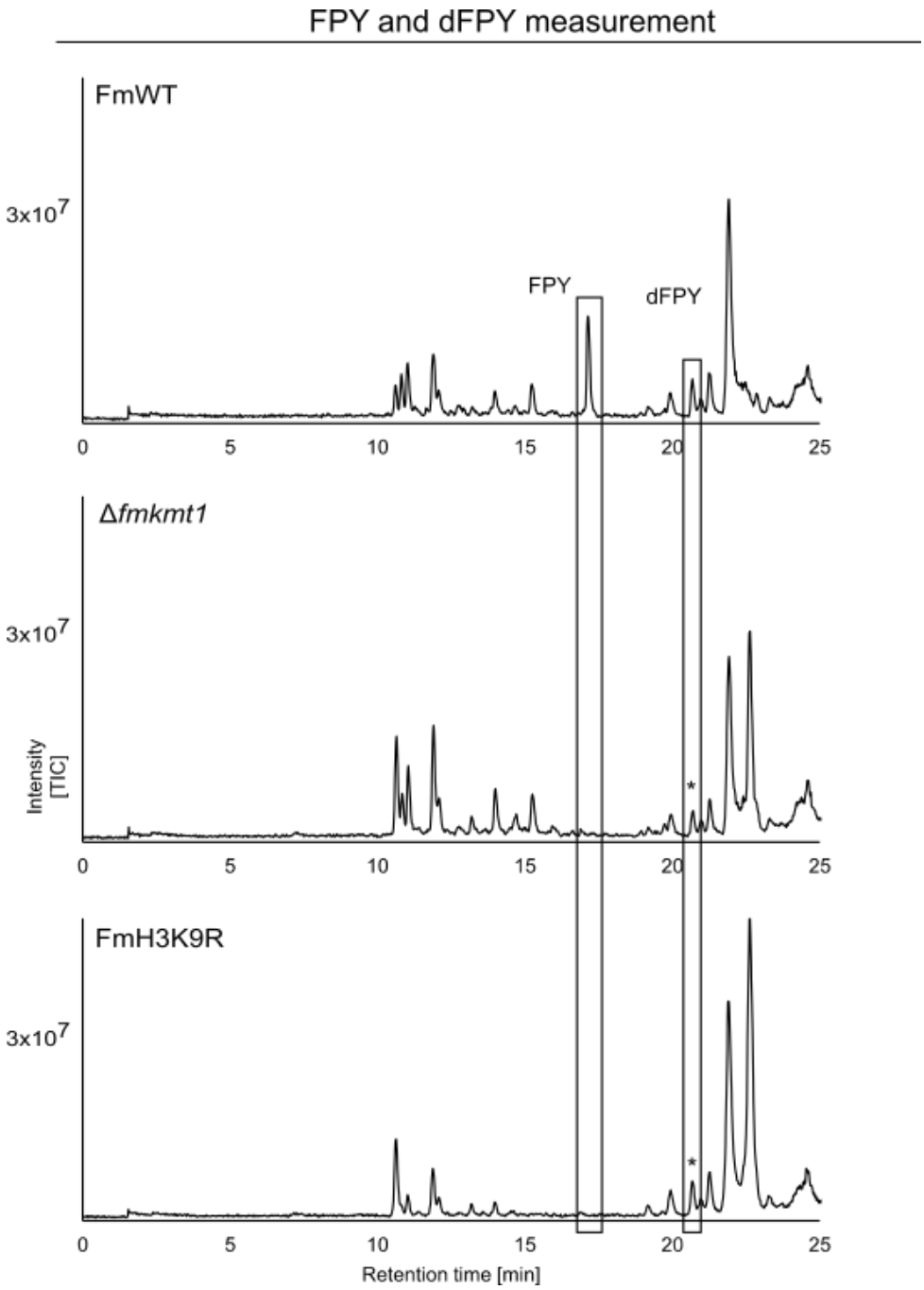

Figure S10: HPLC-HRMS chromatograms of FPY and dFPY production in the Δ*fmkmt1* deletion and FmH3K9R point mutation strain compared to the wild-type strain (FmWT). The *F. mangiferae* wild-type strain (FmWT), Δ*fmkmt1* T13 and FmH3K9R T24 were cultivated in FPY-inducing media for 7 days at 30°C. Experiments were performed in technical triplicates. Peaks for FPY and dFPY (boxed) are present in FmWT but absent from Δ*fmkmt1* and FmH3K9R cultures.The asterisk (*) indicates that the observed signal in the Δ*fmkmt1* and FmH3K9R chromatogram with a similar retention time as dFPY is distinct from dFPY, because the signal has a different mass. TIC chromatograms (positive ESI-mode) range from m/z 100-1,000.

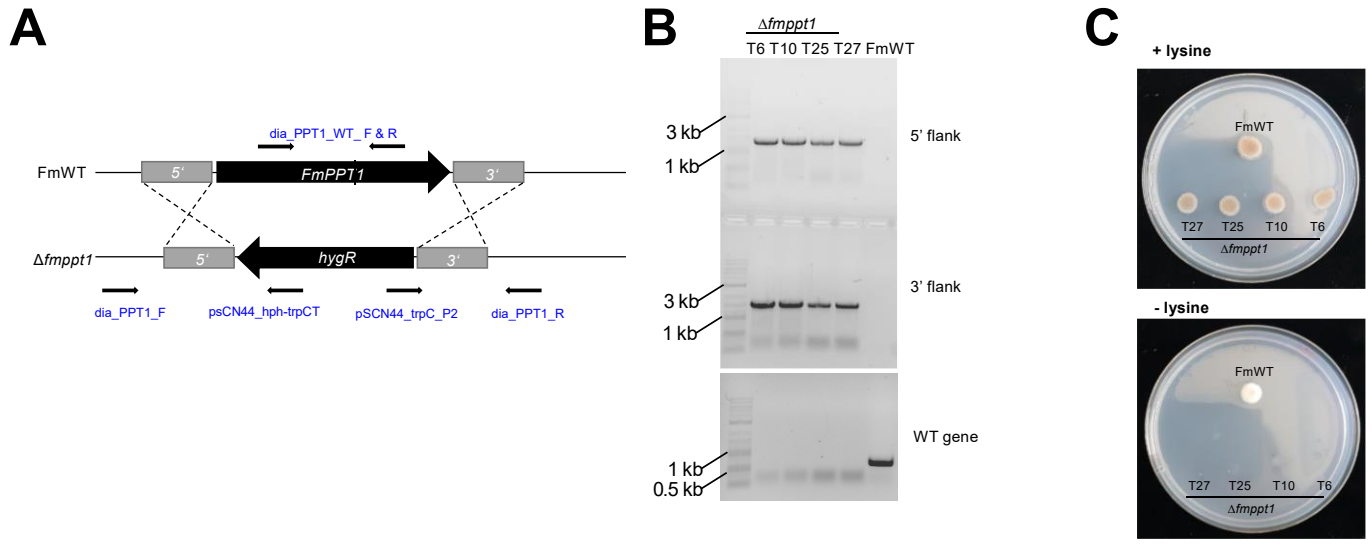

Figure S11: Strategy and verification of Δ*fmppt1* deletion. (A) Deletion and verification strategy of Δ*fmppt1* mutants. Primer pairs for diagnostic PCRs are shown in blue. **(B)** Verification of *in situ* deletion of *FmPPT1 via* homologous recombination with the hygR cassette. Homologous integration was verified by the presence of the upstream region (5' flank) with the primers Dia_FmPPT1_F//pCSN44_hph-trpCT and the downstream region (3' flank) by Dia_FmPPT1_R//pCSN44_trpC_P2. Absence of the wild-type gene was verified using the primer pair Dia_WTPPT1_F//R in the case of four independent transformants i.e., Δ*fmppt1* T6, T10, T25 and T27. FmWT gDNA was used as positive control for the wild-type gene, while it served as negative control for correct integration of the resistance cassette. As size marker 1 kb Plus DNA ladder (NEB) was used. **(C)** Lysine auxotrophy test of Δ*fmppt1*. To further verify presence of positive Δ*fmppt1* strains, growth of FmWT and the respective Δ*fmppt1* strains was assessed on synthetic solid media with (+ lysine) and without (- lysine). As expected, Δ*fmppt1* strains did not grow on media without lysine.

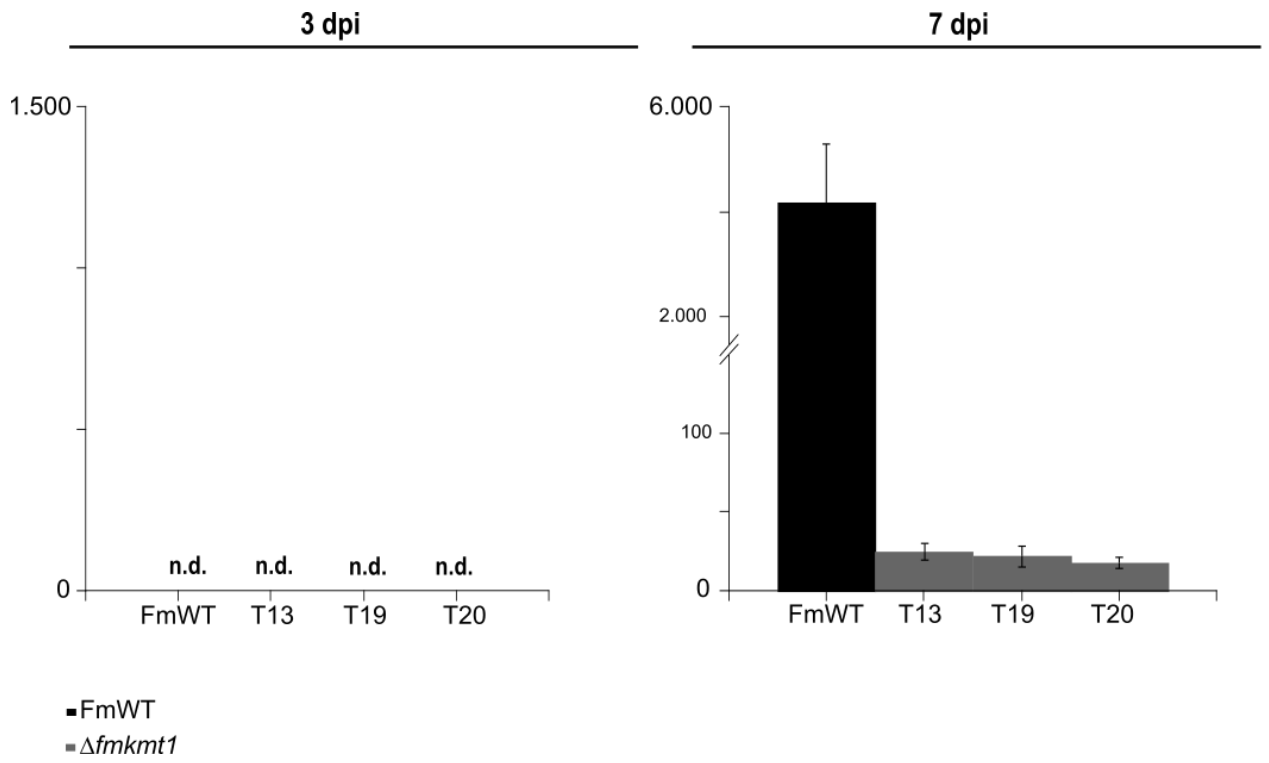

Figure S12: Quantification of fusapyrone (FPY) and deoxyfusapyrone (dFPY) production in *Fusarium mangiferae* 3 and 7 days post inoculation (dpi). The *F. mangiferae* wild-type strain (FmWT), and three independent Δ*fmkmt1* mutants were cultivated for 7 days in liquid ICI supplemented with 6 mM $NaNO_3$ at 30 °C. 1 mL aliquots were taken 3 as well as 7 days post inoculation and analyzed *via* HPLC-HRMS. Experiments were performed in technical triplicates and biological duplicates. Mean values and standard deviations are shown in the diagram. n.d., not detected in the supernatant.

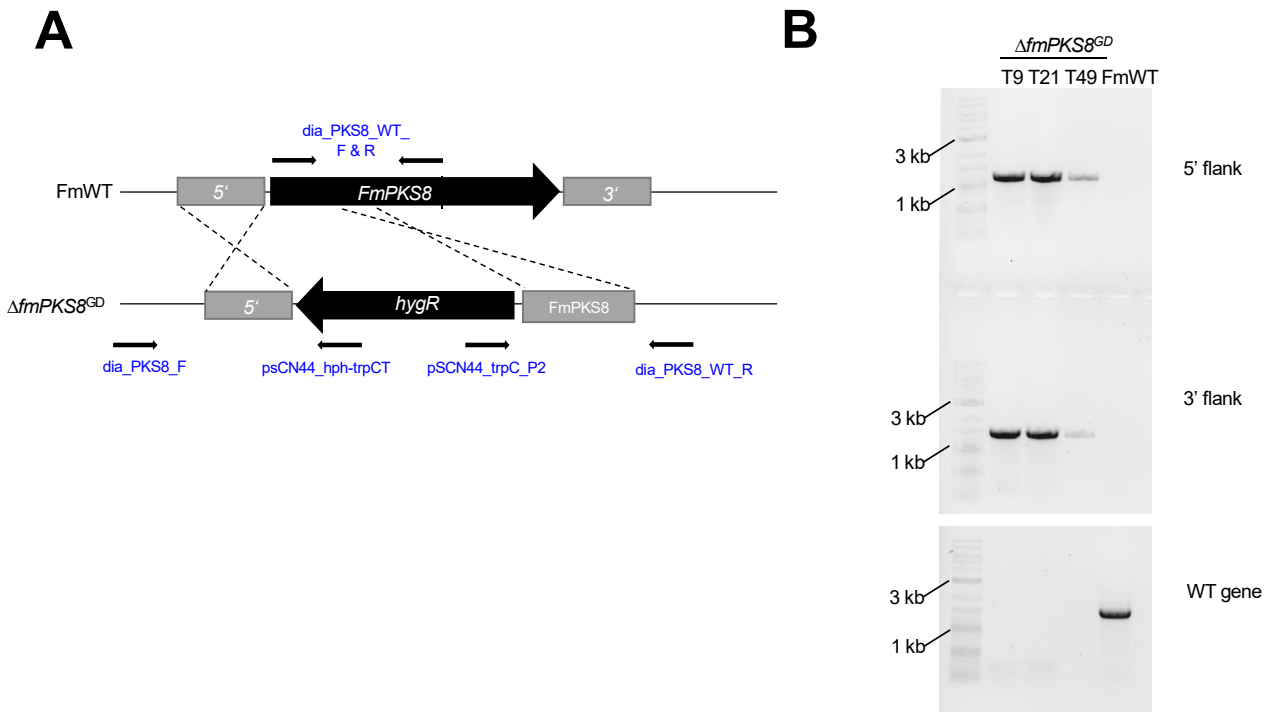

Figure S13: Strategy and verification of Δ*PKS8* disruption by diagnostic PCR. (A) Disruption and verification strategy of Δ*fmPKS8* mutants. Primer pairs for diagnostic PCRs are shown in blue. **(B)** Disruption of Δ*fmPKS8 via* homologous recombination of the hygR cassette. Homologous integration was verified by the presence of the upstream region (5' flank) with the primers Dia_FmPKS8_F//pCSN44_hph-trpCT and the downstream region (3' flank) with Dia_FmPKS8_R//pCSN44_trpC_P2. Absence of the wild-type gene was checked by Dia_WTPKS8_F//R for three independent transformants i.e., Δ*fmPKS8* T9, T21 and T49. FmWT gDNA was used as positive control for the wild-type gene, while it served as negative control for correct integration of the resistance cassette. As size marker 1 kb Plus DNA ladder (NEB) was used.

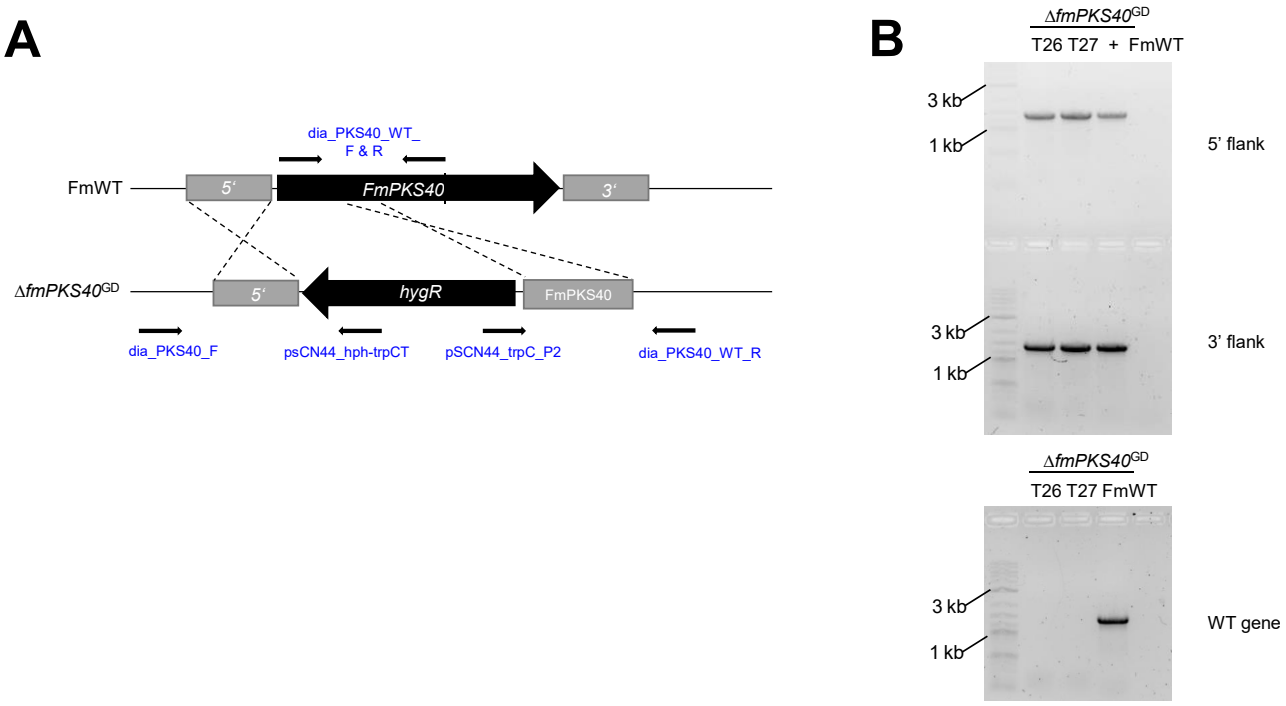

Figure S14: Strategy and verification of Δ*PKS40* disruption by diagnostic PCR. **(A)** Disruption strategy and i*n situ* verification of Δ*fmPKS40* mutants. Primer pairs for diagnostic PCRs are depicted in blue. **(B)** Homologous recombination with the hygR cassette was applied for the disruption and generation of Δ*fmPKS40* strains. Homologous integration events were verified by the presence of the upstream region (5' flank) with the primers Dia_PKS40_F//pCSN44_hph-trpCT and the downstream region (3' flank) using Dia_FmPKS40_R//pCSN44_trpC_P2. Absence of the wild-type gene was checked by Dia_WTFmPKS40_F//R for two independent transformants i.e., Δ*fmPKS40* T26 and T27. For 5' and 3' as positive control (+) Δ*fmPKS40* gDNA prior single spore isolation was used, while for wild-type gene diagnostic PCR FmWT gDNA served as positive + control. As size marker 1 kb Plus DNA ladder (NEB) was used.

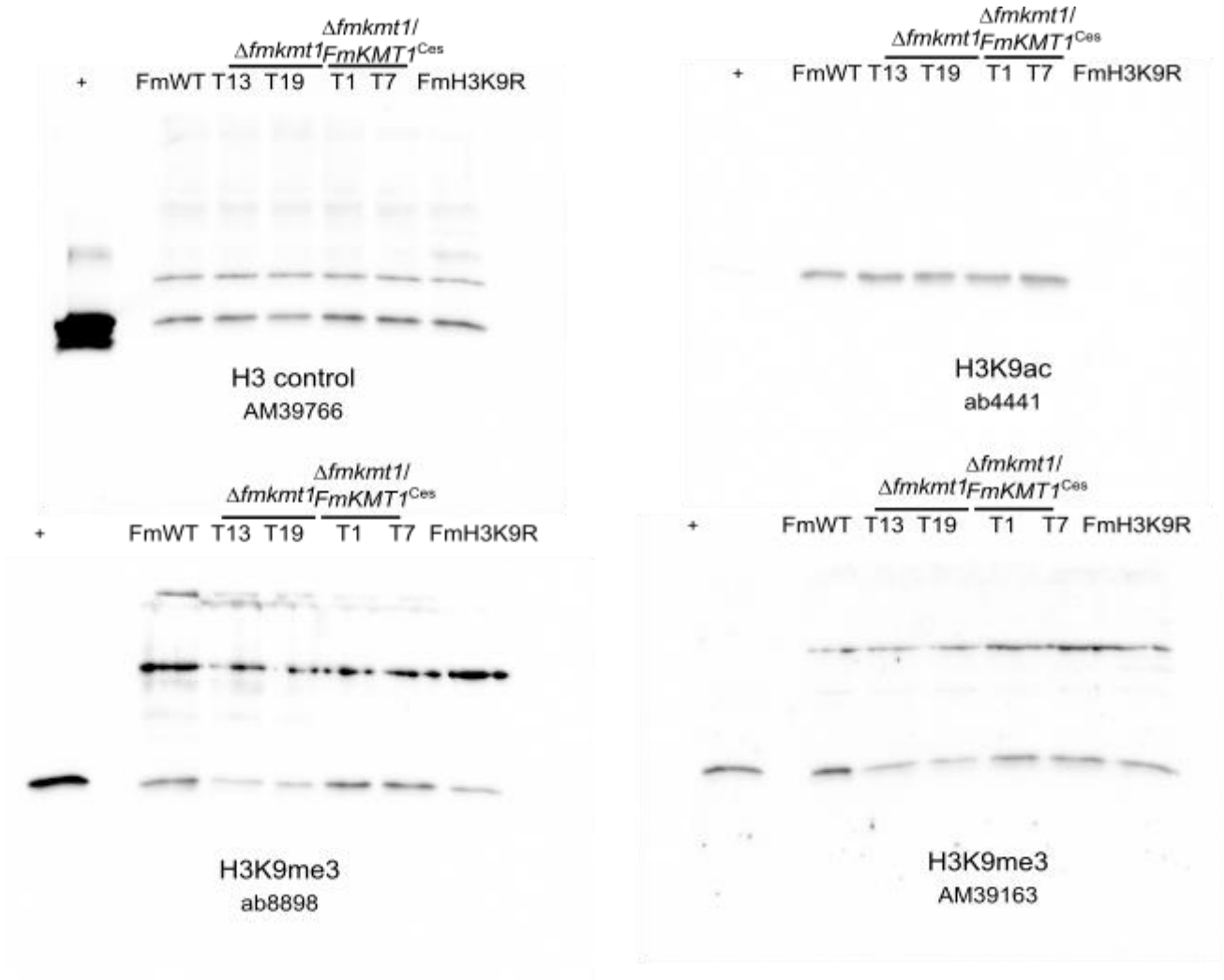

Figure S15: Loss of FmKmt1 and H3K9R point mutation results in overall reduced H3K9me3 in *Fusarium mangiferae*. For western blot analysis, the *F. mangiferae* wild-type strain (FmWT), the Δ*fmkmt1*, complemented Δ*fmkmt1*/*FmKMT1*^{Ces} and H3K9R strains were grown in liquid ICI medium supplemented with 120 mM $NaNO_3$ for 4 days. Roughly 50 µg of total proteins were separated on a SDS gel. For determination of overall H3K9me3 levels, two different anti-H3K9me3-specific antibodies (AB, Abcam; AM, Active Motif) were applied. For the quantification of H3K9ac levels an anti-H3K9ac-specific antibody was used, while anti-H3 C-term-specific antibody was used for referencing. As positive (+) control histones from calf thymus were used.

Table S1: List of primers used in this work. Introduced overhangs required for yeast recombinational cloning are written in lowercase letters. Primers are designed with * also bind in *F. mangiferae* genome. Primer designed with ᵅ bind also in *F. proliferatum* ET1, *F. proliferatum* NRRL62905 and *F. verticillioides* M3125 genomes.

Gene ID	Primer ID	Primer sequence
	Primer used for plasmid generation	
FMAN_07768	FmKMT1_5F	gccagggttttcccagtcacgacgGGTGATCAAGTTTGAATCTCGG
	FmKMT1_5R	ttaacgttactgaaatctccaacCCTCTCTAGTAACACTGCACA
	FmKMT1_3F	caatatcatcttctgtctccgacACTTCTTACAAGGGAGGTAGG
	FmKMT1_3R	ataacaatttcacacaggaaacagcCCATGGTCATGAAGCTCTTTGC
/	FmCIL_tgluc	ATACATCTTATCTACATACGTCACCACAAGAACTTCCTGC
/	Geni-Tgluc_R	ACCCCTTCCCCCCAACAAGATATCATCATGCAACATGCATGTACTG
/	GeniF	GTCGGAGACAGAAGATGATATTGAAGGAGCCAACAAAACACAGTTCCGACCAC
/	Tgluc-nat1R	ATCTTGTTGGGGGGAAGGGGT
/	Tgluc_F2	CGTATGTAGATAAGATGTATG
FMAN_09280	FmPPT1_5F	gccagggttttcccagtcacgacgAGTACAGTAGCAATGCCTCAGCG
	FmPPT1_5R	ttaacgttactgaaatctccaacTGCAACTATTGCCTTGGAATGCC
	FmPPT1_3F	caatatcatcttctgtctccgacCTCATAGGCTAGTTACATCTCGC
	FmPPT1_3R	aacaatttcacacaggaaacagcACTTGCTACCTGCAGAACAAGCC
FMAN_15223	FmPKS8_5F	aacgccagggttttcccagtcacgGGCAAGAACTCAGGTATTGACGG
	FmPKS8_5R	tccacttaacgttactgaaatctccCTGGGGTTCCACCACATCTTTACC

	FmPKS8_3F	ccttcaatatcatcttctgtctccgTCTTAGCCCTTTGTCTATGTATCG
	FmPKS8_3R	cggataacaatttcacacaggaaacaCCACCAAGTAAGCTCGGTTCTCC
	FmPKS8GD_3F	tcaatatcatcttctgtctccgacTCTCATTGAAGAACTCCGTGCTCC
	FmPKS8GD_3R	aacaatttcacacaggaaacagcACGAAGGACTTGTTTCCAGTGAACC
FMAN_00008	FmPKS40_5F	gccagggttttcccagtcacgacgGGTCCAGGCTAAATACACAACTGG
	FmPKS40_5R	cttaacgttactgaaatctccaacCCGATGAAAACACCAGTGTTTGTTCC
	FmPKS40GD_3F	ttcaatatcatcttctgtctccgacCGAGGCTGGAACCAATATATCACC
	FmPKS40GD_3R	ataacaatttcacacaggaaacagcCTCATAGAGCTGTCGAAATGAGGTC
FMAN_12510	Histone3_Mut_1F	ccagggttttcccagtcacgacgCACTGGTAGTGTATGGTGATGTGC
	Histone3_Mut_2R	catacatcttatctacatacgTTAGTTGCGCTCGCCTCGGAGGC
	Histone3_Mut_4F	tcaatAtcatcttctgtcTCCGACGCGATATCACGTATGGGTATTCAGG
	Histone3_Mut_4R	actggccgtcgttttacaaGTGAAGAAGACGGTGATCCAGG
	Histone3_Mut_K9R_1R	CGGTGGACcTGCGGGCGGTCTGC
	Histone3_Mut_K9R_2F	GCAGACCGCCCGCAgGTCCACCG
/	Splitmarker_hph_F	CGTTGCAAGACCTGCCTGAA
/	Splitmarker_hph_R	GGATGCCTCCGCTCGAAGTA
	Primers for diagnostic PCR	
FMAN_07768	Dia_FmKMT1_F	TGAATGGTTATAGACGGGAGCC

	Dia_FmKMT1_R	GCAAAGAGCTTCATGACCATGG
	Dia_WTKMT1_F	AACGCCATTTCTACTTCCACGG
	Dia_WTKMT1_R	TGGGCAGTCTATACTACAGG
genR	Gen_seq1	GAGCCTGAATGTTGAGTGG
	Gen_seq3	CAGCCGATTGTCTGTTGTGC
	genR_split_F	GGGAAGGGACTGGCTGCTATTG
FMAN_09280	Dia_FmPPT1_F	GACGAAAAGAAAGACGGAGAGG
	Dia_FmPPT1_R	TACCTTGCCCTACATAGTACG
	Dia_WTPPT1_F	CAAGACCAAAGACCTCACATCC
	Dia_WTPPT1_R	GGCAAACTTGTGCATCTCTAGG
FMAN_15223	Dia_FmPKS8_F	GGCTGGTGAGCATGTTACAATAGG
	Dia_FmPKS8_R	CATCGCCCTTAGCATACGAGC
	Dia_WTPKS8_F	GGTGTCTTCACAGGTCAAGG
	Dia_WTPKS8_R	CCGCAAAGAGGATCTCAGTTCC
FMAN_00008	Dia_FmPKS40_F	AGCCTCACTCTTGGCAAATCC
	Dia_WTPKS40_F	CAGACTCTGGTGGTATCTTTGCC
	Dia_WTPKS40_R	ACCATGACTTGGTCAATCTCGC
/	pCSN44-trpC_P2	GTGATCCGCCTGGACGACTAAACC
/	pCSN44-hph-trpC-T	GGAATAGAGTAGATGCCGACCGG
FMAN_12510	FmH3_dia_R	GCTAGCTGCAGTTTCACACTG
	FmH3_dia_F	CACAACGCGTCGAATATGATCC
Primer used for sequencing		

FMAN_07768	Dia_WTFmKMT1_F	AACGCCATTTCTACTTCCACGG
	Dia_WTFmKMT1_R	TGGGCAGTCTATACTACAGG
/	pRS426_seq	GCCATTCAGGCTGCGCAACTG
/	Bcgluc_seq	GGGTCCATGCTAATACTTATGTAC
/	Gen_seq1	GAGCCTGAATGTTGAGTGG
/	Gen_seq2	CTCGTGCTTTACGGTATCGC
/	Gen_seq3	CAGCCGATTGTCTGTTGTGC
/	URA3_F	GCTGACATTGGTAATACAGTC
/	Tgluc-HiF	CATACGTACATCTGATTTGACAACC
/	Hph-F	GTCGGAGACAGAAGATGATATTGAAGGAGC
/	Hph-R	GTTGGAGATTTCAGTAACGTTAAGTGGAT
/	trpC-P	CCTCCACTAGCTCCAGCCAAGCCC
FMAN_12510	H3_Mut_Seq1	GGAGAGCTTAAGTACGAGTG
	H3_Mut_Seq2	CTGTGTCATTGAATGAGCC
	H3_Mut_Seq3	GACAGCAAATTCGCCATTGG
	H3_Mut_Seq4	CAACAACAACTATCATCAACC
	H3_Mut_Seq5	TGCTCTCCAGGAGTCCGTCG
	H3_Mut_Seq6	TCAGTCACGCTCTCTAATCC
	H3_Mut_Seq7	GTCATGTGGTCTCCGATCAGG
Primers for semi-quantitative and RT-qPCR		
cDNA verification		

FFUJ_02611	cDNA_check_Actin_F	GTATGTGCAAGGCCGGTTTCG
	cDNA_check_Actin_R	GAGACCAGGGTACATGGTGG
*Housekeeping genes**		
FFUJ_02611	Actin_F	CCACCATGTACCCTGGTCTCTCC
	Actin_R	AATGGAACCACCGATCCAGACGG
FFUJ_07385	ß-TUB_F	GAGGCAGTACGATGGCATGCG
	ß-TUB_R	GGTAATCTGCGTCTTCAGCAGCTTCG
FFUJ_13490	GPD_F	GCCTCTGAGGGTGACCTCAAGG
	GPD_R	CGTTGTCGTACCAGGAGACCAGC
FmKMT1		
FMAN_07768	FmKmt1_F	TGCTAAAGGCCACAGAACGCC
	FmKmt1_R	CTGGGAGTGTTGAGTGAGTCGGA
PKS genes		
FMAN_01974	FmPKS2_F	GCTGATGGCGGTTGAGTTGAGG
	FmPKS2_R	CGAGCTTCGCATCTCAGCGAC
FMAN_08330	FmPKS5_F	GATCCGGGTTTCACCATGCCG
	FmPKS5_R	TCTGCTGCTCTATCCAGAGCCG
FMAN_15223	FmPKS8_F	CTCCAGTCCGAGGACGACAGC
	FmPKS8_R	ACATTGGTGTCAAGCTCCTCTGGC
FMAN_13212	FmPKS12_F	CACTTACTGCGATTGAGTTGCGGC
	FmPKS12_R	CAACGTCTCTCAACGACGGTGC
FMAN_15195	FmPKS17_F	ATGGTGTCGACTCACTGGTTGC

	FmPKS17_R	AATCTCGCTAGCCAACGCTCG
FMAN_00008	FmPKS40_F	TTGATTCCCTCGTCGCAGTCG
	FmPKS40_R	AGCCAGTTCAGCCAACTCTTCC
FMAN_09800	FmPKS43_F	TGCTTAAGCCTGTGGAGGACCTTG
	FmPKS43_R	CCAAGGACGTCCAGCGTCC
FFB14_11413[α]	FfPKS40_F	CCTTGTTGCGGTCGAGTTGC

Table S2: Presence of SM genes and linked products in *F. mangiferae*

Gene	Gene ID	Product	Reference
Non-ribosomal peptide synthetases			
FmNRPS1	FMAN_06841	malonichrom	(Oide et al., 2014)
FmNRPS2	FMAN_02774	ferricrocin (intracellular sideophores)	(Tobiasen et al., 2007; Oide et al., 2014)
FmNRPS3	FMAN_07066		
FmNRPS4	FMAN_10843		
FmNRPS6	FMAN_13615	fusarinine (extracellular sideophores)	(Varga et al., 2005)
FmNRPS10	FMAN_05062		
FmNRPS11	FMAN_13817		
FmNRPS12	FMAN_06437		
FmNRPS13	FMAN_04011		
FmNRPS20	FMAN_06958		
FmNRPS21	FMAN_00090		
FmNRPS22	FMAN_12971	beauvericin	(Xu et al., 2008; Zhang et al., 2013; Niehaus et al., 2016)
FmNRPS23	FMAN_15153		
FmNRPS24	FMAN_08295		
FmNRPS25	FMAN_08343		
FmNRPS26	FMAN_08290		
FmNRPS34	FMAN_03675	fusaric acid	(Brown et al., 2012; Niehaus et al., 2014; Studt et al., 2016)
Polyketide synthases			
FmPKS1/NRPS	FMAN_03782	trichosetin	(Hansen et al., 2015)
FmPKS2	FMAN_01974		
FmPKS3	FMAN_03378	fusarubins	(Studt et al., 2012)
FmPKS4	FMAN_06935	bikaverin	(Linnemannstöns et al., 2002b)
FmPKS5	FMAN_08330		
FmPKS6	FMAN_03664	fusaric acid	(Brown et al., 2012; Niehaus et al., 2014; Studt et al., 2016)
FmPKS7	FMAN_09265		
FmPKS8	FMAN_15223		
FmPKS9/NRPS	FMAN_06335		
FmPKS10/NRPS	FMAN_12219	fusarin C (pseudogene and abrogated SMGC)	(Brown et al., 2012)

FmPKS12	FMAN_13212		
FmPKS13	FMAN_15141	gibepyrones	(Janevska et al., 2016)
FmPKS14	FMAN_13912		
FmPKS17	FMAN_15195		
FmPKS18	FMAN_15205		
FmPKS20/NRPS	FMAN_11871		
FmPKS38	FMAN_02337		
FmPKS40	FMAN_00008	fusapyrone / deoxyfusapyrone	**This study**
FmPKS43	FMAN_09800		
Dimethylallytryptophane synthases			
FmDMATS1	FMAN_13061	r-*N*-DMAT	(Arndt et al., 2017)
FmDMATS2	FMAN_06887		
FmDMATS3	FMAN_06328		
FmDMATS4	FMAN_06531		
Terpene cyclases			
FmDTC1-1	FMAN_08250	gibberellins	(Tudzynski and Hölter, 1998)
FmTrTC1	FMAN_05579		
FmTeTC1	FMAN_14945	phytoene	(Linnemannstöns et al., 2002a)
FmSTC1	FMAN_02036		
FmSTC2	FMAN_01129		
FmSTC3	FMAN_03293	(+)-eremophilene	(Burkhardt et al., 2016)
FmSTC4	FMAN_13218	(+)-koraiol	(Brock et al., 2013)
FmSTC5	FMAN_14887	(–)-guaia-6,10(14)-diene	(Burkhardt et al., 2016)
FmSTC6	FMAN_11750	(–)-α-acorenol	(Brock et al., 2013)
FmSTC7	FMAN_16004		
FmSTC8	FMAN_12837		
FmSTC9	FMAN_06479		

Table 3: RT-qPCR raw data from FPY SMGC co-expression studies

	Gene ID	60 mM glutamine		6 mM glutamine		120 mM $NaNO_3$		6 mM $NaNO_3$	
Housekeeping genes									
Actin	FMAN_04166	/	21.34	21.52	21.88	20.41	20.40	18.02	18.03
Tubulin	FMAN_05925	26.50	26.12	26.54	26.59	24.38	24.53	23.12	23.14
GPD	FMAN_07563	19.60	19.90	20.53	20.72	18.94	19.07	17.37	17.41
Investigated genes/ Putative cluster genes									
	FMAN_00001	22.43	22.33	23.08	22.90	22.17	22.15	20.17	20.14
	FMAN_00002	35.20	36.36	24.52	24.63	33.08	34.31	17.52	17.46
	FMAN_00003	36.99	36.96	26.22	26.55	36.25	36.31	19.31	19.44
	FMAN_00004	28.14	28.34	25.07	25.08	28.06	28.11	18.15	18.13
	FMAN_00005	/	/	27.60	27.77	39.50	/	20.81	20.70
	FMAN_00006	36.55	38.33	24.29	24.49	37.30	/	18.32	17.64
	FMAN_00007	39.81	/	27.03	27.38	/	34.84	18.32	18.52
	FMAN_00008	36.98	38.26	25.40	25.26	37.60	36.34	17.60	17.50
	FMAN_00009	36.82	33.73	35.19	33.37	36.53	34.44	31.27	31.23
	FMAN_000010	31.21	31.39	31.18	31.09	32.55	32.32	29.19	/
	FMAN_000011	27.30	27.24	32.81	32.61	28.27	28.58	29.31	29.60
	FMAN_000012	33.75	32.42	33.37	32.93	32.76	32.55	32.03	32.52
	FMAN_000013	29.51	29.51	34.34	33.65	30.20	30.51	32.05	32.70

Table 4: Detailed analysis of putative *fmfpy* SMGC

Gene ID	Length (bp)	Number of amino acids	InterPro annotation	Family type (F), Domains (D) and motifs (M)	Predicted function
FmFPY1 (FMAN_00002)	1666	519	IPR001128 IPR002402 IPR002974	Cytochrome P450 (F) Cytochrome P450, E-class, group II (F) Cytochrome P450, E-class, CYP52 (F)	Related to cytochrome P450 alkane hydroxylase
FmFPY2 (FMAN_00003)	1190	349	IPR000683 IPR004104	Oxidoreductase, N-terminal (D) Gfo/Idh/MocA-like oxidoreductase, C-terminal (D)	Related to dehydrogenases and related proteins
FmFPY3 (FMAN_00004)	2157	597	IPR011701 IPR020846	Major facilitator superfamily (F) Major facilitator superfamily domain (D)	Related to multidrug transporter
FmFPY4 (FMAN_00005)	1110	369			FAD dependent oxidoreductase
FmFPY5 (FMAN_00006)	834	218	IPR005645	Serine hydrolase FSH (D)	FSH1 domain-containing protein
FmFPY6 (FMAN_00007)	1696	546	IPR002213	UDP-glucuronosyl/UDP-glucosyltransferase (F)	Related to UDP-glucosyl transferase family protein
FmFPY7 (FMAN_00008)	7580	2474	IPR009081 IPR013149 IPR013217 IPR013968 IPR014030 IPR014031 IPR014043 IPR020806	Phosphopantetheine binding ACP domain (D) Alcohol dehydrogenase, C-terminal (D) Methyltransferase type 12 Polyketide synthase, ketoreductase domain (D) Beta-ketoacyl synthase, N-terminal (D) Beta-ketoacyl synthase, C-terminal (D) Acyl transferase Polyketide synthase, phosphopantetheine-binding	FmPKS40

IPR020807	domain (D)
IPR020841	Polyketide synthase, dehydratase domain
IPR020843	Polyketide synthase, beta-ketoacyl synthase domain (D)
IPR032821	Polyketide synthase, enoylreductase domain (D)
	Polyketide synthase, C-terminal extension (D)

Table 5: Comparison of *FPY* SMBGC with other members of the FFC

Predicted gene function	*F. mangiferae* MRC7560	*F. fujikuroi* B14	*F. proliferatum ET1*	*F. proliferatum* NRRL62905	*F. verticillioides* M3125
Unknown	FMAN_00001	FFB14_11405	/	FPRN_00001	/
Cytochrome P450 alkane hydroxylase	**FMAN_00002**	**FFB14_11407**	**FPRO_00007**	/	/
Dehydrogenase	**FMAN_00003**	**FFB14_11408**	**FPRO_00008**	/	/
Multidrug transporter	**FMAN_00004**	**FFB14_11409**	**FPRO_00009**	/	**FVEG_09964**
FAD dependent oxidoreductase	**FMAN_00005**	**FFB14_11410**	**FPRO_00010**	/	**FVEG_09963**
FSH1 domain-containing protein	**FMAN_00006**	**FFB14_11411**	**FPRO_00011**	/	/
UDP-glucosyl transferase family protein	**FMAN_00007**	**FFB14_11412**	**FPRO_00012**	/	/
PKS40	**FMAN_00008**	**FFB14_11413**	**FPRO_00013**	**FPRN_00002**	**FVEG_16698T0**
Cellulose binding protein	FMAN_00009	/	/	/	/
Mfs-multidrug-resistance transporter	FMAN_00010	FFB14_11414	FPRO_00014	FPRN_00003	FVEG_09958
Unknown	FMAN_00011	FFB14_11415	FPRO_00015	FPRN_00004	/
Transporter	FMAN_00012	FFB14_11416	FPRO_00016	FPRN_00005	/
Zn(2)-C6 fungal-type domain-containing protein	FMAN_00013	FFB14_11417	FPRO_00017	FPRN_00006	/

References

Arndt, B., Janevska, S., Schmid, R., Hübner, F., Tudzynski, B., and Humpf, H.-U. (2017). A Fungal N-Dimethylallyltryptophan Metabolite from Fusarium fujikuroi. *ChemBioChem* 18, 899–904. doi:10.1002/cbic.201600691.

Blum, M., Chang, H. Y., Chuguransky, S., Grego, T., Kandasaamy, S., Mitchell, A., et al. (2021). The InterPro protein families and domains database: 20 years on. *Nucleic acids research* 49, D344–D354. doi:10.1093/nar/gkaa977.

Brock, N. L., Huss, K., Tudzynski, B., and Dickschat, J. S. (2013). Genetic Dissection of Sesquiterpene Biosynthesis by Fusarium fujikuroi . *ChemBioChem* 14, 311–315. doi:10.1002/cbic.201200695.

Brown, D. W., Butchko, R. A. E., Busman, M., and Proctor, R. H. (2012). Identification of gene clusters associated with fusaric acid, fusarin, and perithecial pigment production in Fusarium verticillioides. *Fungal Genetics and Biology* 49, 521–532. doi:10.1016/j.fgb.2012.05.010.

Burkhardt, I., Siemon, T., Henrot, M., Studt, L., Rösler, S., Tudzynski, B., et al. (2016). Mechanistic Characterisation of Two Sesquiterpene Cyclases from the Plant Pathogenic Fungus Fusarium fujikuroi. *Angewandte Chemie* 128, 8890–8893. doi:10.1002/ange.201603782.

Hansen, F. T., Gardiner, D. M., Lysøe, E., Fuertes, P. R., Tudzynski, B., Wiemann, P., et al. (2015). An update to polyketide synthase and non-ribosomal synthetase genes and nomenclature in Fusarium. *Fungal Genetics and Biology* 75, 20–29. doi:10.1016/j.fgb.2014.12.004.

Janevska, S., Arndt, B., Niehaus, E. M., Burkhardt, I., Rösler, S. M., Brock, N. L., et al. (2016). Gibepyrone biosynthesis in the rice pathogen Fusarium fujikuroi is facilitated by a small polyketide synthase gene cluster. *Journal of Biological Chemistry* 291, 27403–27420. doi:10.1074/jbc.M116.753053.

Linnemannstöns, P., Prado, M. M., Fernández-Martín, R., Tudzynski, B., and Avalos, J. (2002a). A carotenoid biosynthesis gene cluster in Fusarium fujikuroi: The genes carB and carRA. *Molecular Genetics and Genomics* 267, 593–602. doi:10.1007/s00438-002-0690-5.

Linnemannstöns, P., Schulte, J., del Mar Prado, M., Proctor, R. H., Avalos, J., and Tudzynski, B. (2002b). The polyketide synthase gene pks4 from Gibberella fujikuroi encodes a key enzyme in the biosynthesis of the red pigment bikaverin. *Fungal Genetics and Biology* 37, 134–148. Available at: www.academicpress.com.

Niehaus, E. M., von Bargen, K. W., Espino, J. J., Pfannmüller, A., Humpf, H. U., and Tudzynski, B. (2014). Characterization of the fusaric acid gene cluster in Fusarium fujikuroi. *Applied Microbiology and Biotechnology* 98, 1749–1762. doi:10.1007/s00253-013-5453-1.

Niehaus, E.-M., Studt, L., von Bargen, K. W., Kummer, W., Humpf, H.-U., Reuter, G., et al. (2016). Sound of silence: The beauvericin cluster in Fusarium fujikuroi is controlled by cluster-specific and global regulators mediated by H3K27 modification. *Environmental Microbiology* 18, 4282–4302. doi:10.1111/1462-2920.13576.

Oide, S., Berthiller, F., Wiesenberger, G., Adam, G., and Turgeon, B. G. (2014). Individual and combined roles of malonichrome, ferricrocin, and TAFC siderophores in Fusarium graminearum pathogenic and sexual development. *Frontiers in Microbiology* 5. doi:10.3389/fmicb.2014.00759.

Studt, L., Janevska, S., Niehaus, E. M., Burkhardt, I., Arndt, B., Sieber, C. M. K., et al. (2016). Two separate key enzymes and two pathway-specific transcription factors are involved in fusaric acid biosynthesis in Fusarium fujikuroi. *Environmental Microbiology* 18, 936–956. doi:10.1111/1462-2920.13150.

Studt, L., Wiemann, P., Kleigrewe, K., Humpf, H., and Tudzynski, B. (2012). Biosynthesis of Fusarubins Accounts for Pigmentation of Fusarium fujikuroi Perithecia. *Applied and Environmental Microbiology* 78, 4468–4480. doi:10.1128/AEM.00823-12.

Tobiasen, C., Aahman, J., Ravnholt, K. S., Bjerrum, M. J., Grell, M. N., and Giese, H. (2007). Nonribosomal peptide synthetase (NPS) genes in Fusarium graminearum, F. culmorum and F. pseudograminearium and identification of NPS2 as the producer of ferricrocin. *Current Genetics* 51, 43–58. doi:10.1007/s00294-006-0103-0.

Tudzynski, B., and Hölter, K. (1998). Gibberellin Biosynthetic Pathway in Gibberella fujikuroi: Evidence for a Gene Cluster. *Fungal Genetics and Biology* 25, 157–170.

Varga, J., Kocsube, S., Toth, B., and Mesterhazy, A. (2005). NONRIBOSOMAL PEPTIDE SYNTHETASE GENES IN THE GENOME OF FUSARIUM GRAMINEARUM, CAUSATIVE AGENT OF WHEAT HEAD BLIGHT. *Acta Biologica Hungarica* 56, 375–388.

Xu, Y., Orozco, R., Wijeratne, E. M. K., Gunatilaka, A. A. L., Stock, S. P., and Molnár, I. (2008). Biosynthesis of the Cyclooligomer Depsipeptide Beauvericin, a Virulence Factor of the Entomopathogenic Fungus Beauveria bassiana. *Chemistry and Biology* 15, 898–907. doi:10.1016/j.chembiol.2008.07.011.

Zhang, T., Zhuo, Y., Jia, X. P., Liu, J. T., Gao, H., Song, F. H., et al. (2013). Cloning and characterization of the gene cluster required for beauvericin biosynthesis in Fusarium proliferatum. *Science China Life Sciences* 56, 628–637. doi:10.1007/s11427-013-4505-1.